Received 23 December 2023; revised 15 February 2024; accepted 24 February 2024. Date of publication 29 February 2024; date of current version 22 May 2024.
The review of this article was arranged by Editor Y. Kikuchi.

Digital Object Identifier 10.1109/JEDS.2024.3371455

Enhancement of Selectivity for Chemical Mechanical Polishing by Ultra-High-Dose C and Si Ion Implantation

S. YUAN [1], K. OMORI [1], T. YAMAGUCHI [1], T. IDE [2], S. MURANAKA [1], AND M. INOUE [1]

1 Process Production Technology Division, Production and Technology Unit, Renesas Electronics Corporation, Hitachinaka 312-8504, Ibaraki, Japan
2 Device Technology Division, Production and Technology Unit, Renesas Electronics Corporation, Hitachinaka 312-8504, Ibaraki, Japan

CORRESPONDING AUTHOR: S. YUAN (e-mail: shuo.yuan.vt@renesas.com)

This work was supported by the Renesas Electronics Corporation.

ABSTRACT The selectivity of chemical mechanical polishing (CMP) is successfully enhanced due to the modification of the film surface by ultra-high-dose ion implantation for the first time. The removal rate (RR) of CMP for SiO_2 and Si_3N_4 films was changed by implanted ions. On the other hand, polycrystalline silicon (poly-Si) films had no change regardless of ion implantation. When C^+ is implanted at 3×10^{16} ions/cm^2 into SiO_2, the RR decreases by about 40% compared with that without implantation. However, no significant change was observed after the implantation of C^+ at 1×10^{16} ions/cm^2 or Si^+ to SiO_2 and poly-Si films. New findings about CMP mechanism that are against Borst's Langmuir-Hinshelwood model have been made when the film is modified by using high-dose implantation.

INDEX TERMS Implantation, material modification, surface modification, CMP, selectivity, RMG, gate-last.

I. INTRODUCTION

Low power system-on-a-chip (SoC) products have gained increasing popularity in mobile and hand-held consumer electronic markets as silicon technology scaling allows more functionality and complexity to be packed into a single chip per Moore's Law. It was a significant breakthrough in the 45 nm process by using a "high-k" (High-k) material called hafnium to replace the transistor's silicon dioxide gate dielectric, and by using new metals to replace the negative channel metal-oxide semiconductor (NMOS) and positive channel metal-oxide semiconductor (PMOS) poly-Si gate electrodes [1], [2]. For micro controller unit (MCU), 28 nm and 40 nm embedded devices are the most common processes in practical use. As the rapid advances in the microelectronics industry demand a continuous decrease in the device size together with the complex structure and materials such as High-k/Metal-gate, high selective polishing is required in the CMP for manufacturability. For example, in mass-productive manufacturing, devices with different gate heights and sizes, such as metal oxide nitride oxide silicon (MONOS), metal oxide semiconductor (MOS), and input/output (I/O) structures are all embedded in one plane.

In the gate-last approach, also known as replacement metal gate (RMG), high-k dielectrics do not need to go through high temperature steps, which helps to minimize V_T shift and improve device reliability [3]. Even though high-k/metal-gate gate-last process has been mass produced for years, one of the concerns often brought up is the process complexity of CMP [4].

Figure 1 shows a typical RMG process flow, which involves gate stack formation followed by a) a pre-metal dielectric (PMD) deposition, b) an PMD CMP step to planarize the dielectric film and expose dummy poly-Si gate, an etch step that removes the dummy poly-Si gate, followed by work function materials deposition, c) aluminum (Al) metal deposition and d) Al CMP [5]. Because of the tight dimensional requirements for gate structures (both within die and within wafer) a lack of process control for post CMP film thickness can lead to integration issues such as gate resistance variation, poor gate fill, raised source/drain exposure, *etc.* that can adversely affect device performance [6]. A good process control capability for minimizing within die (WID), within wafer (WIW) and wafer-to-wafer (WTW) thickness variations is therefore necessary to achieve good

© 2024 The Authors. This work is licensed under a Creative Commons Attribution-NonCommercial-NoDerivatives 4.0 License.
For more information, see https://creativecommons.org/licenses/by-nc-nd/4.0/

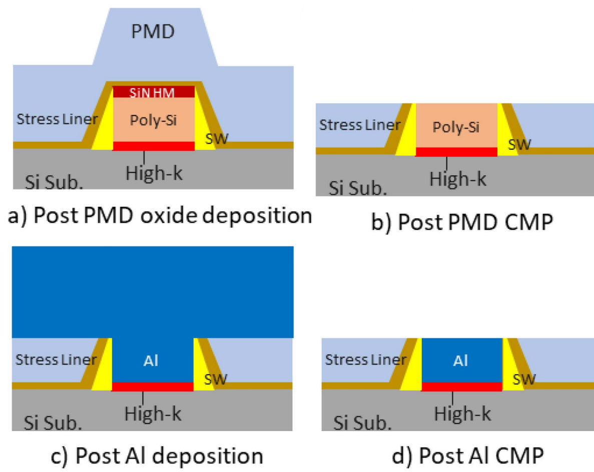

FIGURE 1. **Process flow of replacement metal gate (RMG).**

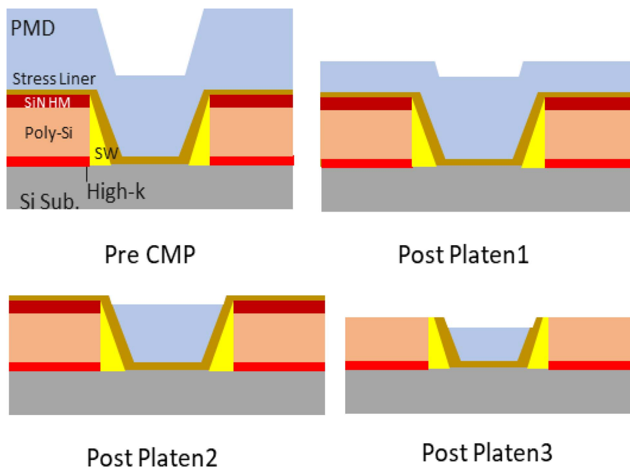

FIGURE 2. **Schematic representation of oxide removal in field area during pre-metal dielectric CMP.**

device performance and reliability. As shown in Figure 2, a three-platen CMP was developed to address the good performance requirements in PMD CMP. On platen1, the PMD bulk dielectric film is removed. On platen 2, the gate area is polished further, to stop on nitride (SiN) gate cap, by a fixed abrasive (FA) process. On platen 3, nitride in the gate area is completely removed to expose the poly-Si gate. However, as shown in Figure 3, at the last step, nitride, oxide, and poly-Si are polished at the same time in different gate height and size, which makes selectivity of CMP to each film more critical. For example, when the RR for SiO_2 is higher than Si_3N_4 and poly-Si, PMD recess around gate takes place and possibly cause photo misalignment issues due to the destructive interference of the beam at certain depth [7]. In order to improve the process stability of RMG, suppressing the RR of CMP for SiO_2 and poly-Si while raising RR for Si_3N_4 is the key.

Since more accurate control of the RR for each material is required, improving the selectivity of CMP slurry to SiO_2, Si_3N_4, and poly-Si is significant [8]. When reducing

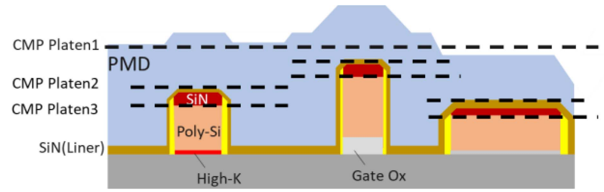

FIGURE 3. **Different patterns embedded in a same plane.**

such local dishing and erosion of device patterns through planarization, it is necessary to intentionally enhance the selectivity of CMP, and slurries are generally expected to be effective [9]. CMP slurries have been utilized in processes to planarize structures which consist of several different materials. Chemical reagents in the CMP slurry react with the wafer surface being polished, forming a chemically modified top layer with desirable properties compared to the initial wafer surface [10], [11]. The selectivity to different films in CMP is commonly determined by the type of slurry and depends on the addition of pH regulators, oxidizers, or stabilizers [12], [13]. White et al. [14] and Kozhukh and Guo [15] advocated that the key parameter was the attractive interaction of the abrasive particles with SiO_2 wafer realizing by the gap of their zeta potentials. This ought to be an important parameter, however, their proposal only deals with the approaching step of abrasive particles to the surface of a SiO_2 wafer, which is insufficient to describe polishing mechanism of SiO_2 CMP. High selectivity is almost obtained by three factors, pH at around 7, electronegative surfactant and CeO_2 abrasive [16]. At pH 7, zeta potential of SiO_2 is negative [17] whereas that of Si_3N_4 is positive [18], so that electronegative surfactants adhere only to the Si_3N_4 and interrupt reaction with the abrasive. There is also a report about that changing the adhesion force of the abrasive particle to the SiO_2 wafer was the most important parameter to enhance the RR for SiO_2 [19]. Silica abrasive, which is very sensitive to the pH, shows abruptly reduced reaction rate as the pH decreases, is suitable as a solution for increasing the rate for Si_3N_4 while suppressing the rate for SiO_2 film. Ideally, as a stopping material, the RR for poly-Si should be almost negligible. While bare silicon is highly dependent on chemical factors such as pH, poly-Si is highly dependent on mechanical factors [20]. For this reason, silica is also an abrasive that is suitable for poly-Si gate exposure process. Much research has been made regarding changing selectivity by adding additives to modify the top layer.

On the other hand, it has been reported that the wet and dry etching rates for SiO_2, Si_3N_4, and photo-resist film can be changed by material modification using the ion implantation technique [21], [22], [23]. Ion implantation breaks the molecular bonds in materials and the wet or dry etching rate might change. Ion implantation is also able to offer the advantage of localized modification within the wafer plane when used in conjunction with a hard mask. Furthermore, it has been also demonstrated that

TABLE 1. CMP process parameters.

Items	Values
platen speed (rpm)	75
head speed (rpm)	71
Z1 pressure (kPa)	44
Z2 pressure (kPa)	22
Z3 pressure (kPa)	24
Z4 pressure (kPa)	24
Z5 pressure (kPa)	24
Z6 pressure (kPa)	59

high-dose ion implantation can change the binding energy of Si-O and Si-N [24]. However, the effect of the material modification with ion implantation on CMP has almost not been researched.

In this study, we investigate a novel method to chemically modify the material by using high-dose implantation. The effect of material modification on RR of CMP by using C^+ and Si^+ high-dose low-energy ion implantation for SiO_2, Si_3N_4, and poly-Si film is reported, and it has a high potential for resolving local dishing and erosion due to local steps of device patterns through planarization.

II. EXPERIMENTAL PROCEDURES

In this experiment, three types of 300 mm blanket wafers were prepared, respectively. *A.* 200 nm thick SiO_2 films for PMD material were deposited by chemical vapor deposition (CVD). *B.* 20 nm thick Si_3N_4 films for nitride gate cap material were deposited by plasma enhanced CVD. *C.* 100 nm thick polycrystalline silicon (poly-Si) films for dummy gate material were deposited by Low-pressure CVD. Film thicknesses were measured by ellipsometry after deposition (which is also before CMP) and after CMP. The ion implantation for material modification was carried out by ultra-high-current ion implanter. The implantation energy to control the depth profile of implanted ion was determined by using the Monte Carlo simulation. Implantation energies into SiO_2 and Si_3N_4 film were adjusted to have almost the same projected range (Rp) of 10 nm. C^+ was implanted at 2.0 keV into SiO_2, Si_3N_4, and poly-Si films, respectively. Si^+ was implanted at 4.0 keV into SiO_2, 2.0 keV into Si_3N_4, and poly-Si films, respectively. The implantation dose was changed with a range from 1.0×10^{16} to 3×10^{16} ions/cm^2. SiO_2 films densified by using rapid thermal annealing (RTA) at 500 °C in 1 minute were prepared after C^+ implantation from 1.0×10^{16} to 3×10^{16} ions/cm^2 at 2.0 keV. All CMP processes were performed on hard pads using colloidal silica-based slurry. The CMP process parameters are shown in Table 1 and 5 zones (Z1, Z2, Z3, Z4, Z5) on 300 mm profile is illustrated in Figure 4. RRs were obtained by measuring

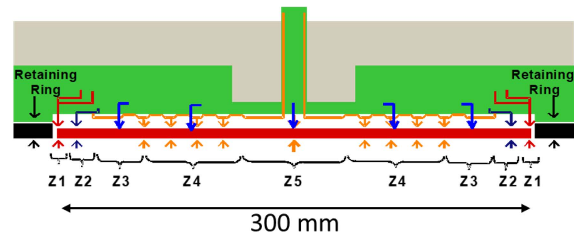

FIGURE 4. CMP zone distribution image.

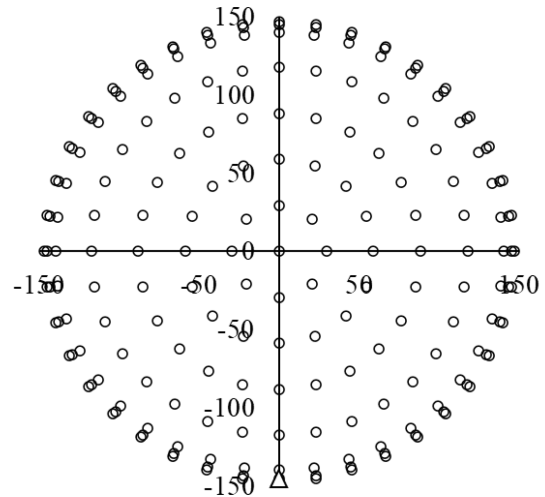

FIGURE 5. Thickness measurement sites.

the removed film thickness before the CMP process (pre-thickness) and after CMP process (post-thickness). These measurements are done at 201 sites on the wafer as shown in Figure 5 (3 mm at the wafer edge are excluded due to edge effect). The RR is calculated as the average of the 201 sites on the wafer divided by the constant polishing time applied in the design of experiments (DOE). In order to assure the authenticity of RR, uniformity was optimized to $\sigma<3\%$. The RR in the depth direction is defined as step-by-step polishing on films. In order to understand the mechanism for the change in the RR of SiO_2, Si_3N_4, and poly-Si films by C^+ and Si^+ implantation, binding energy was evaluated using X-ray photoelectron spectroscopy (XPS).

III. RESULTS & DISCUSSIONS

A. SiO_2 FILM

Figure 6(a) and (b) show the dependency of simulated implantation depth profile with a dose of 3×10^{16} ions/cm^2, energy for C^+ at 2.0 keV, Si^+ at 4.0 keV, and RR of C^+ or Si^+ implanted SiO_2 film with a dose ranging from 1×10^{16} to 3×10^{16} ions/cm^2 at 2.0 keV and 4.0 keV, respectively. The curve of peak value at 10 nm in Figure 6(a), is Rp of C^+ implantation at 2.0 keV, and that in Figure 6(b), is Rp of Si^+ implantation at 4.0 keV. In Figure 6(a), implanted C^+ distributes from the surface to 21 nm and a peak seems around 10nm in depth. For 1×10^{16} ions/cm^2 implanted SiO_2 film, the RR of 0.54 nm/s shows no change in depth from the surface to 50 nm. On the other hand, for SiO_2 film

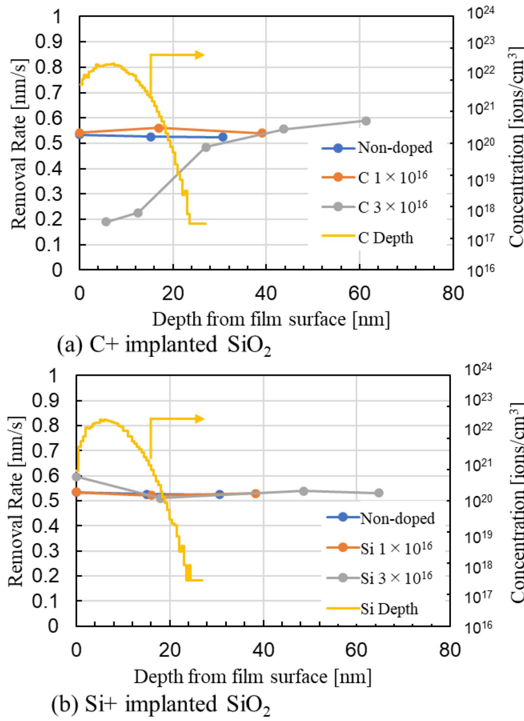

FIGURE 6. Dependency of RR and dose concentration for SiO_2 with (a) C^+ implanted at 2.0 keV, $1\sim3\times10^{16}$ ions/cm^2 and (b) Si^+ implanted at 4.0 keV, $1\sim3\times10^{16}$ ions/cm^2.

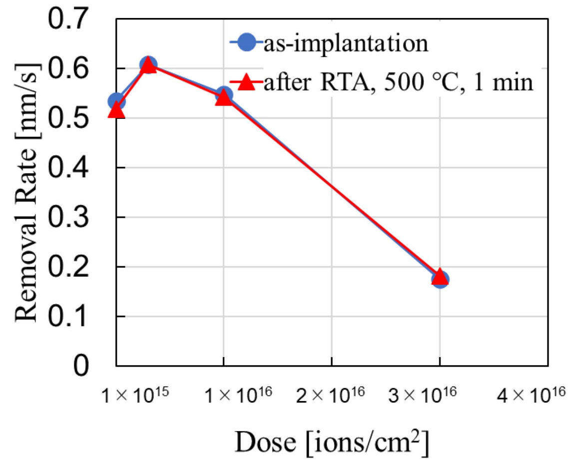

FIGURE 7. Relationship between RR and implantation dose with C^+ at 2.0 keV, $1\times10^{15}\sim3\times10^{16}$ ions/cm^2 for as-implantation SiO_2 and SiO_2 after RTA 500 °C in 1 min.

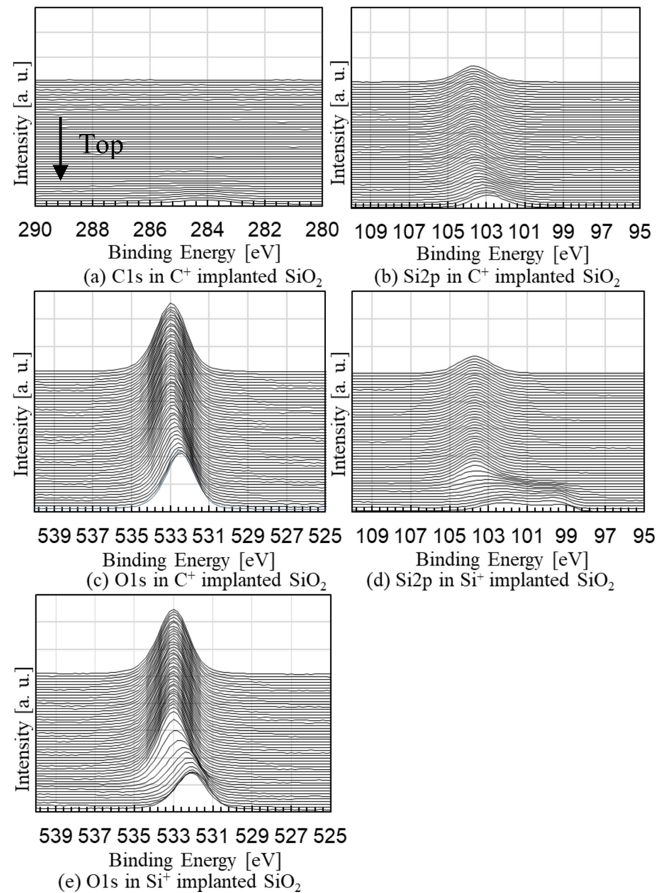

FIGURE 8. XPS spectra of C^+ and Si^+ implanted SiO_2.

with 3×10^{16} ions/cm^2, the RR is 0.20 nm/s on the surface, then, gradually increases to 0.21 nm/s at 12 nm deep, and drastically rises to 0.54 nm/s in depth over 40 nm. This suggests that the fluctuation of RR for C^+ implanted SiO_2 film is related to high-dose implantation. However, according to Figure 6(b), for Si^+ implanted SiO_2 films, the RR shows no change even in a high dose of 3×10^{16} ions/cm^2 and the RR of 0.54 nm/s is stable from the surface to 50 nm in depth.

Figure 7 shows the relationship of RR and dose in a range from 3×10^{15} ions/cm^2 to 3×10^{16} ions/cm^2 for as-implanted SiO_2 and SiO_2 after RTA at 500 °C in 1 minute. The RR After RTA process showed no change compared to that of as-implantation. It was reported that new SiC compounds were generated after RTA process, which resulted in low wet etching rate [24].

In order to understand the binding energy of C^+ and Si^+ implanted SiO_2 films, XPS spectra of C 1s, Si 2p, and O 1s in C^+ and Si^+ implanted SiO_2 film is shown in Figure 8(a)-(c) and Figure 8(d)-(e), respectively. According to Figure 8(a), C 1s binding-energy peak is stable at 284.6 eV, and no peak shift of C 1s is observed. In (b) and (c), although Si 2p and O 1s slightly shift from 103.6 eV and 533.2 eV to the low energy side on the surface, which can be explained by the XPS neutralization, no peak shift of binding energy is observed in a bulk. Thus, no carbon compound, such as Si-C or Si-O-C, in SiO_2 film with the C^+ implantation is generated. Figure 8 (d) and (e) show the binding energy of Si 2p and O 1s in Si^+ implanted SiO_2 film. A sub-peak of Si 2p appears at 99.0 eV and O1s slightly shifts from 532.9 eV to 531.8 eV in ion-implanted layers. It can be assumed that implanted Si^+ generates dangling bonds and resides in the film as the interstitial Si. However, the O-Si-O bond is still stable.

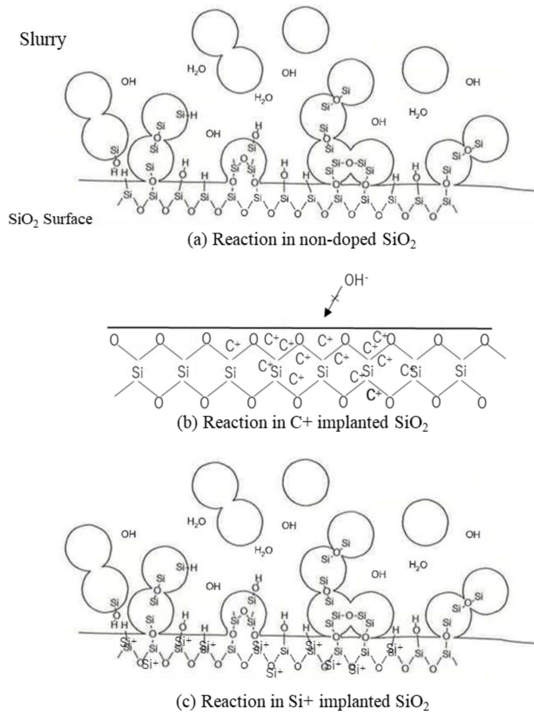

FIGURE 9. Chemical reaction model in implanted SiO_2.

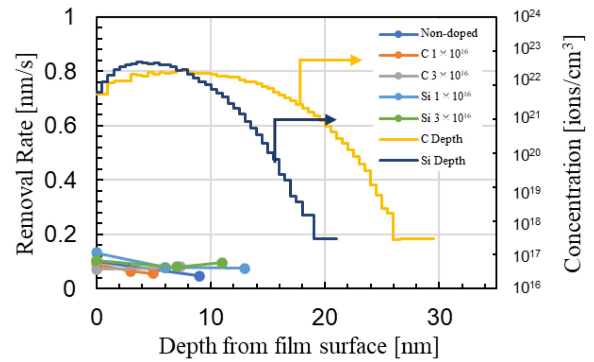

FIGURE 10. Dependency of RR and dose concentration for poly-Si with C^+ and Si^+ implanted at 2.0 keV, $1{\sim}3\times10^{16}$ ions/cm^2.

The mechanism of the RR change can be considered, as shown in Figure 9. In Figure 9(a), the chemical reaction that takes place between the SiO_2 film surface and silica slurry is commonly explained by Cook [25] and Izumitani et al. [26]. OH^- or $(OH)^{2-}$ from slurry attacks the O-Si-O bond and forms a hydration layer. Finally, it can be mechanically removed. However, as shown in Figure 9(b), C^+ with 3×10^{16} ions/cm^2 might form a hydrophobic block layer to prevent forming the hydration layer from OH^- and $(OH)^{2-}$ at O-Si-O interface. Therefore, the RR slows down due to the suppression of the chemical reaction. As a result, it can be considered that the insufficient C^+ block-layer with the dose of 1×10^{16} ions/cm^2 results in no influence on the RR.

Borst et al. proposed a two-step Langmuir-Hinshelwood model [27] which consisted of the chemical step and mechanical one, as one of the models of CMP [28]. At the first step, modification of a substrate surface will be caused by chemical effects. At the second step, mechanical removals of the modified portions of the surface will ensue by abrasives [29]. The following simplified form approximately represents the model RR,

$$(\text{Model RR}) \propto \frac{k_1}{1+\frac{k_1}{k_1+k_2}} \tag{1}$$

where k_1 and k_2 are coefficients correspond to the rate of the chemical contribution and that of the mechanical one, respectively. In this study, high-dose implantation can be expected to correspond to k_1 because film surface is modified, and new chemical compounds is possibly generated.

Here, in order to cancel out the chemical additive factors and simplify the comparison, ratio between the model of implanted and non-doped films is introduced, which is able to be written to:

$$(\text{Ratio RR}) = \frac{(\text{Model RR})_{imp}}{(\text{Model RR})_{non}} \tag{2}$$

where $(\text{Model RR})_{imp}$ is the RR for implanted materials, $(\text{Model RR})_{non}$ is that for non-doped materials. Since no mechanical factors were modified, (2) could be written to:

$$(\text{Ratio RR}) \propto \frac{k_{1imp}}{k_{1non}} \tag{3}$$

where k_{1imp} is the chemical factor of implanted films, k_{1non} is the chemical factor of non-doped films. Here, for implanted SiO_2, it is assumed that block layer derived from implanted C dominated the ration of RR.

B. POLY-SI FILM

Figure 10 shows the RR on C^+ and Si^+ implanted poly-Si film and the simulated ion depth profile for implantation. The curves of peak value at 10 nm are Rp of C^+ implantation at 2.0 keV and Rp of Si^+ implantation at 4.0 keV. The RR of silica slurry is originally very low and almost no change is observed by implanted at 1×10^{16} ions/cm^2 ~ 3×10^{16} ions/cm^2. According to XPS measurement shown in Figure 11(a)-(c), Si 2p at 99.0 eV, which is related to Si-Si bonds, remains in both C^+ and Si^+ implanted films, and no binding energy shift by C^+ and Si^+ was observed in the poly-Si film. These results show that no chemical reactions occurred in poly-Si films. Mechanical factors such as abrasive, pad, and pad conditioner were not changed, therefore, high dose implantation gives no influence on RR for poly-Si film.

Here, when the polishing mechanism extremely depends on the mechanical factor, equation (2) is able to be written to:

$$(\text{Ratio RR}) \propto k_2 \tag{4}$$

which also matches the investigated research [16]. Besides, good stopping property is able to be expected that it can be applied to RMG process.

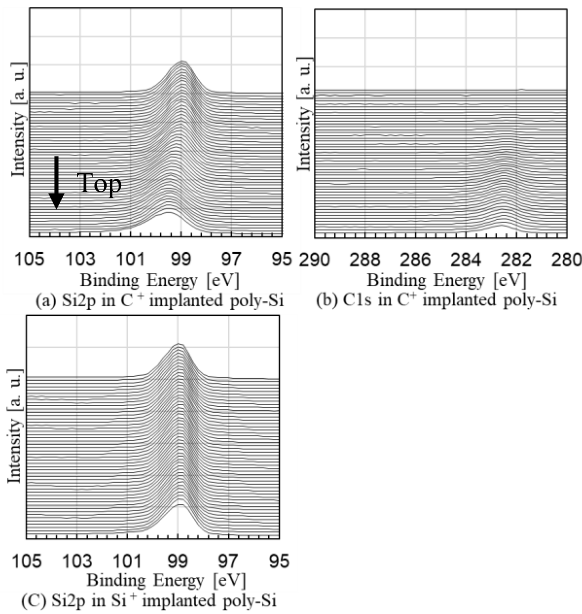

FIGURE 11. XPS spectra of C^+ and Si^+ implanted poly-Si.

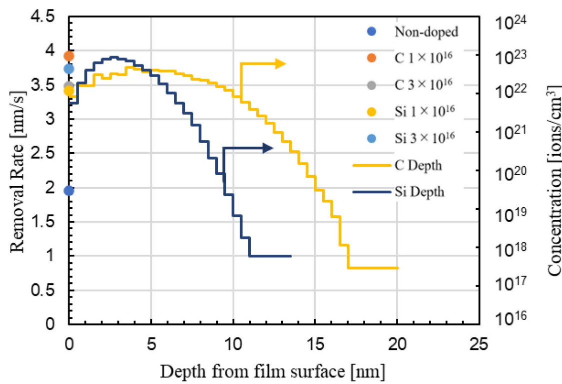

FIGURE 12. Dependency of RR and dose concentration for Si_3N_4 with C^+ and Si^+ implanted at 2.0 keV, $1\sim3\times10^{16}$ ions/cm^2.

C. Si_3N_4 FILM

Figure 12 shows the dependency of the RR on implanted Si_3N_4 film and the simulated ion depth profile for implantation. The curves of peak value at 10 nm are Rp of C^+ implantation at 2.0 keV and Rp of Si^+ implantation at 2.0 keV. Since only 20 nm of Si_3N_4 film was able to be deposited, the RR in depth was only plotted for first CMP, namely, the removal amount (R. A.) of Si_3N_4 film by the first CMP was almost 20nm. Plots at surface depth of 0 nm show the RR. between 0 nm and 20 nm. The RR increases to 3.7 nm/s by implanting C^+ and Si^+ at 1×10^{16} and 3×10^{16} ions/cm^2 compare d to non-doped film with a RR of 2.0 nm/s.

Figure 13 shows the binding energy of C^+ and Si^+ implanted Si_3N_4 film. According to (a), (c) and (e), no binding energy shift was observed for C 1s and N 1s in C^+ implanted Si_3N_4 film. In (b) and (d), binding energy of Si 2p which is generally between 101.5~102.2 eV, slightly shifted

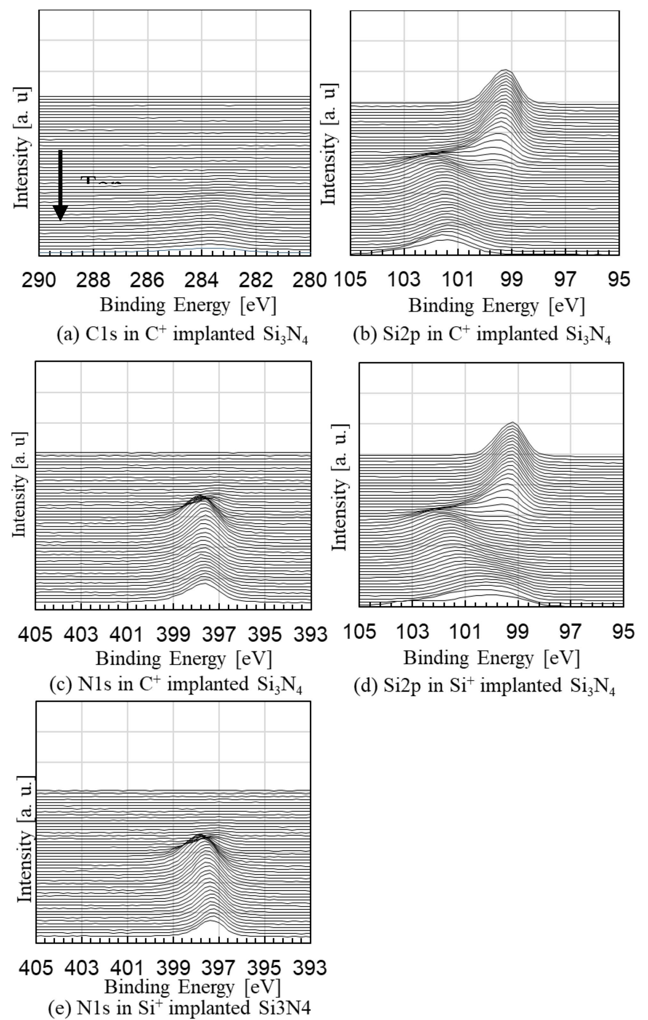

FIGURE 13. XPS spectra of C^+ and Si^+ implanted Si_3N_4.

to lower side under 101.0 eV on the film surface. It is able to be expected that the Si-N binding energy decreased by the additional ion implantation. In (e), no shift of binding energy was observed for N 1s in Si^+ implanted Si_3N_4.

The mechanism of the increment of RR due to ion implantation might be considered as follows:

Toshio et al. showed that the RR was proposed on the basis of the chemical reaction of the Si_3N_4 with chemical additives that were expected to be able to interfere Si-N bond strength stemming from their adsorption on the Si_3N_4 substrate [30]. Since the binding energy of Si 2p decreased on the surface, it can be assumed that implanted C^+ and Si^+ are interstitial C and Si, which also decrease the bond order. The difference in RR between implanted and non-doped Si_3N_4 films is strongly related to the change in the bond order between Si and N. The Si-N binding energy can be decreased on Si_3N_4 surface at low dose such as 1×10^{16} ions/cm^2. It can be considered that RR showed no difference between low dose at 1×10^{16} ions/cm^2 and high dose at 3×10^{16} ions/cm^2 is because that interstitial C and Si saturate at 1×10^{16} ions/cm^2.

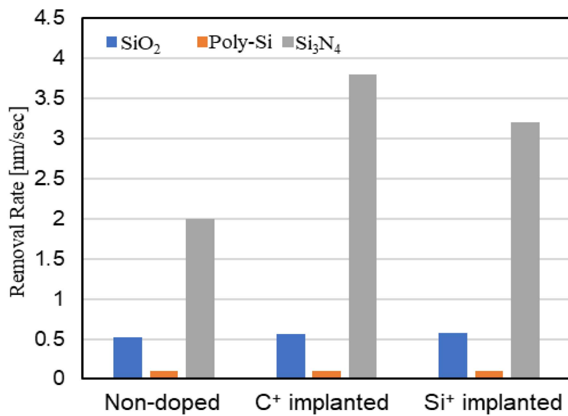

FIGURE 14. Selectivity enhanced by high-dose implantation at 1×10^{16} ions/cm^2.

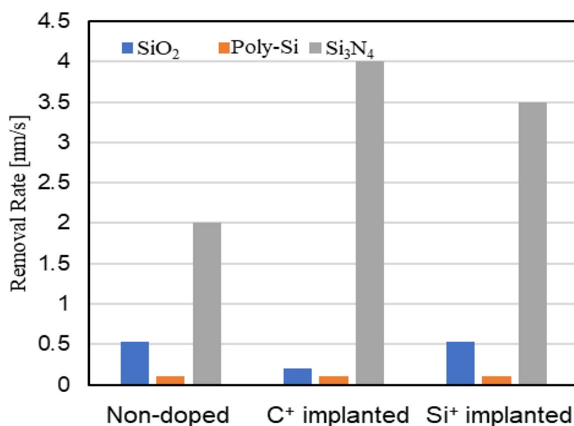

FIGURE 15. Selectivity enhanced by high-dose implantation at 3×10^{16} ions/cm^2.

This result corresponds to equation (3), which different from the case of SiO_2, can be attributed to the block layer derived from implanted C.

D. SUMMARY & FUTURE OUTLOOK

To summarize the RR of each material, Figure 14 shows the selectivity of the RR for SiO_2, poly-Si, and Si_3N_4 at 1×10^{16} ions/cm^2 at a surface depth of 10 nm. Only the RR against Si_3N_4 film increased. This result might be considered that it is not enough to enhance the RR and cause the dishing upon PMD film. Figure 15 shows the selectivity of the RR for SiO_2, poly-Si, and Si_3N_4 at 3×10^{16} ions/cm^2 at a surface depth of 10 nm. C^+ implantation at 3×10^{16} ions/cm^2 decreases the RR for SiO_2 by 40%. However, for poly-Si, the RR has no change. Furthermore, the RR for Si_3N_4 is raised. For Si^+ implantation at 3×10^{16} ions/cm^2, only the RR for Si_3N_4 is raised by 2 times, and for SiO_2 and poly has no change. It has a great potential to enhance the selectivity for CMP by using high-dose implantation. Since this work is only studied with blanket wafer, effects such as the ion concentration at the same surface depth is different for different materials and layout dependency in embedded wafers are still unknow, further studies are needed.

IV. CONCLUDING REMARKS

The CMP RR in ultra-high-dose ion-implanted blanket films is investigated for the first time. The RR for SiO_2 film is down to 40% with C^+ implantation at 3×10^{16} ions/cm^2, which is considered due to a hydrophobic block-layer formation. The RR for SiO_2 with C^+ implantation shows that after RTA process, even with lower dose at 1×10^{16} ions/cm^2, RR could be reduced to the same extent as with high dose at 3×10^{16} ions/cm^2 implanted SiO_2. The RR for Si_3N_4 increases by C^+ implantation. However, the RR for poly-Si has not changed. In the case of Si+ implantation, no change in the RR for poly-Si and SiO_2 was confirmed. The RR only for Si_3N_4 increases up to 40∼50%. High dose implantation gives strong influence more in chemical factors than mechanical factors in SiO_2 film and Si_3N_4 film. Borst's Langmuir-Hinshelwood model is not completely adaptive to material modifications by using high-dose implantation, which can be attributed to different film types.

This novel technique of ultra-high-dose ion implantation to films can enhance the selectivity of CMP for advanced microelectronic devices, and this technique has a high potential for applications to improve poly-Si gate exposure process such as RMG in embedded device processes.

ACKNOWLEDGMENT

The authors thank H. Kai, R. Wada, and T. Kuroi with NISSIN ION EQUIPMENT CO., LTD. for providing the high-dose implantation and discussions.

REFERENCES

[1] K. Mistry et al., "A 45nm logic technology with high-k+metal gate transistors, strained silicon, 9 Cu interconnect layers, 193nm dry patterning, and 100% Pb-free packaging," in *IEDM Tech. Dig.*, 2007, pp. 247–249, doi: 10.1109/IEDM.2007.4418914.
[2] T. Y. Hoffman, "Integrating high-k/metal gates: Gate-first or gate-last?" *Solid State Technol.*, vol. 53, no. 3, pp. 20–21. [Online]. Available: https://sst.semiconductor-digest.com/2010/03/integrating-high-k/
[3] C. Auth, A. Cappellani, J.-S. Chun, and A. Dalis, "45nm high-k + metal gate strain-enhanced transistors," in *Symp. VLSI Dig.*, 2008, p. 128, doi: 10.1109/VLSIT.2008.4588589.
[4] D. Lammers, "Gate first or gate last: Technologist debate high-k," *Semicond. Int.*, vol. 33, pp. 10–13, Mar. 2010. [Online]. Available: https://scsong.wordpress.com/2010/03/10/gate-first-or-gate-last-technologists-debate-high-k-2010-03-10-154115-semiconductor-international/
[5] J. Steigerwald, "Chemical mechanical polish: The enabling technology," in *Proc. IEDM*, 2008, Art. no. 370040, doi: 10.1109/IEDM.2008.4796607.
[6] J. Diao et al., "ILD0 CMP: Technology enabler for high k metal gate in high performance logic devices," in *Proc. IEEE/SEMI Adv. Semicond. Manuf. Conf. (ASMC)*, 2010, pp. 247–250, doi: 10.1109/ASMC.2010.5551458.
[7] T. Park et al., "A novel simple shallow trench isolation (SSTI) technology using high selective CeO_2 slurry and liner SIN as a CMP stopper," in *Proc. Symp. VLSI Technol.*, 1999, pp. 159–160, doi: 10.1109/VLSIT.1999.799392.
[8] S. Suzuki, T. Akatsuka, A. Endou, and K. Sugai, "Study on mechanisms of SiO_2-CMP," in *Proc. ISSM*, 2018, pp. 1–3, doi: 10.1109/ISSM.2018.8651181.

[9] *Planarization and CMP Technical Committee: A Library of CMP Planarization Technology & Application*, Japan Soc. Precis. Eng., Tokyo, Japan, p. 84.
[10] H. Huang et al., "New CMP processes development and challenges for 7nm and beyond," in *Proc. China Semicond. Technol. Int. Conf. (CSTIC)*, Shanghai, China, 2018, pp. 1–5, doi: 10.1109/CSTIC.2018.8369258.
[11] G. B. Shin, V. Korthius, G. Grover, S. Fang, and D. S. Bonig, "Chemical-mechanical polishing," in *Handbook of Semiconductor Manufacturing Technology*, 2nd ed., R. Doering and Y. Nishi, Eds. New York, NY, USA: CRC Press, 2008, Ch. 17. [Online]. Available: https://books.google.co.jp/books?id=PsVVKz_hjBgC&printsec=copyright&redir_esc=y#v=onepage&q&f=false
[12] C. Allain, M. Cloitre, and M. Wafra, "Aggregation and sedimentation in colloidal suspensions," *Phys. Rev. Lett.*, vol. 74, pp. 1478–1481, 1995, doi: 10.1103/PhysRevLett.74.1478.
[13] G. Bahar Basim and B. M. Moudgil, "Slurry design for chemical mechanical polishing," *KONA Powder Particle J.*, vol. 21, pp. 178–184, Sep. 2003, doi: 10.14356/kona.2003020.
[14] M. L. White, L. Jones, and R. Romine, "The mechanism of low pH colloidal silica-based oxide slurries," in *Proc. MRS*, 2010, pp. E04–07, doi: 10.1557/PROC-1249-E04-07.
[15] J. Kozhukh and Y. Guo, "Cationic silica particles in acidic CMP slurries for performance enhancement," in *Proc. CMPUG*, 2017, pp. 1–15.
[16] W. S. Sie, Y. L. Liu, and J. F. Lin, "High-k metal gate poly opening polish at 28nm technology polish rate and selective study," in *Proc. ICPT*, 2014, pp. 183–185, doi: 10.1109/ICPT.2014.7017275.
[17] M. S. Darsillo and S. G. Allen, "Structure precipitated silicates and silicas, production and use in ink jet printing," U.S. Patent 5 827 363, Oct. 1998. [Online]. Available: https://patents.google.com/patent/US5827363A/en
[18] R. A. McCauley, "Ceramic powder useful in the manufacture of green and densified fired ceramic articles," U.S. Patent 5 273 942, Dec. 1993. [Online]. Available: https://patents.justia.com/inventor Ronald-a-mccauley
[19] G. Menk et al., "New polish chemistry and process for improved fixed abrasive CMP performance," in Proc. *Int. Conf. Planarization/CMP Technol.*, Dresden, Germany, 2007, pp. 1–6.
[20] Y.-J. Kang et al., "Effect of slurry pH on poly silicon CMP," in *Proc. Int. Conf. Planarization/CMP Technol.*, 2007, pp. 1–6.
[21] J. R. Conrad, J. L. Radtke, R. A. Dodd, F. J. Worzala, and N. C. Tran, "Plasma source ion-implantation technique for surface modification of materials," *J. Appl. Phys.*, vol. 62, p. 4591, Dec. 1987, doi: 10.1063/1.339055.
[22] E. J. H. Collart et al., "Effects of implant temperature and millisecond annealing on dopant activation and diffusion," in *Proc. AIP Conf.*, 2012, pp. 95–98, doi: 10.1063/1.4766498.
[23] Y. Okuyama et al., "High dose ion implantation into photoresist," *J. Solid State Sci. Technol.*, vol. 125, no. 8, 1978, pp. 1293–1298.
[24] R. Wada, H. Kai, N, Kawakami, J. Sasaki, and T. Kuroi, "The investigation of material modification for SiO_2, Si_3N_4 film and photoresist using high-dose ion implantation technique" in *Proc. 4th IEDM*, 2020, pp. 1–4, doi: 10.1109/EDTM47692.2020.9117807.
[25] L. M. Cook, "Chemical processes in glass polishing" *J. Non-Crystal. Solids*, vol. 120, pp. 152–171, Apr. 1990, doi: 10.1016/0022-3093(90)90200-6.
[26] T. Izumitani, E. Miyade, and S. Adachi, "Chemical durability of optical glass," *J. Non-Crystal. Solids*, vol. 42, nos. 1–3, pp. 569–578, Oct. 1980, doi: 10.1016/0022-3093(80)90056-3.
[27] V. Guerra, "Analytical model of heterogeneous atomic recombination on silicalike surfaces," *IEEE Trans. Plasma Sci.*, vol. 35, no. 5, pp. 1397–1412, Oct. 2007, doi: 10.1109/TPS.2007.902028.
[28] C. L. Borst, D. G. Thakurta, W. N. Gill, and R. J. Gutmann, "Surface kinetics model for SiLK chemical mechanical polishing," *J. Electrochem. Soc.*, vol. 149, no. 2, pp. G118–G127, 2002, doi: 10.1149/1.1431576.
[29] K. Tamai, A. Yasui, H. Morinaga, T. Doi, and S. Kurokawa, "Effect of particle-substrate interaction on the polishing rate," *Proc. ICPT*, 2009, pp. 55–59.
[30] T. Toshio, A. Endou, and K. Sugai, "Novel CMP technology for removal rate control of SiN," in *Proc. ISSM*, 2018, pp. 1–3, doi: 10.1109/ISSM.2018.8651168.